Materials Science and Engineering, 89 (1987) 25–33

Steady State Creep Deformation of Superalloy Inconel 718

YAFANG HAN* and M. C. CHATURVEDI

Department of Mechanical Engineering, University of Manitoba, Winnipeg R3T 2N2 (Canada)

(Received May 14, 1986; in revised form July 11, 1986)

ABSTRACT

The creep deformation mechanism of Inconel 718 superalloy strengthened by coherent ordered disc-shaped body-centred tetragonal (DO_{22}) γ'' phase and coherent spherical f.c.c. ($L1_2$) γ' phase precipitates has been studied in the stress range 620–840 MN m^{-2} and the temperature range 853–943 K. Constant-stress tensile creep tests were used to measure the values of steady state creep rate $\dot{\epsilon}_s$ and the consecutive stress reduction method was used to determine the values of back stress. Transmission electron microscopy was used to measure the particle size of the γ'' and γ' phases and to observe the dislocation structures of crept specimens. It has been found that the values of effective stress exponent n_e and activation energy Q_e expressed by the creep rate equation

$$\dot{\epsilon}_s = A^* \left(\frac{\sigma_a - \sigma_0}{G}\right)^{n_e} \frac{Gb}{kT} \exp\left(-\frac{Q_e}{RT}\right)$$

were between 1.2 and 5.9 and between 250 and 310 kJ mol^{-1} respectively. The values of n_e and Q_e suggest that the creep deformation mechanism changes from diffusional creep at 853–873 K to dislocation power law creep at 943 K in the stress range 620–720 MN m^{-2}. However, at the temperature of 873 K the creep mechanism changes from diffusional or linear creep at applied stresses below 720 MN m^{-2} to dislocation power law creep in the stress range 765–840 MN m^{-2}.

1. INTRODUCTION

The creep mechanisms that operate during elevated temperature deformation of pure metals and solid solution alloys are characterized by the value of the stress exponent n_a in the creep rate equation

$$\dot{\epsilon}_s = A\sigma_a{}^{n_a} \exp\left(-\frac{Q_a}{RT}\right)$$

where $\dot{\epsilon}_s$ is the steady state creep rate, σ_a is the applied stress, Q_a is the activation energy, T is the creep temperature, R is the gas constant and A is a constant. Therefore a determination of the value of the stress exponent n_a can identify a particular creep mechanism that controls the creep deformation in a given stress and temperature region. When $n_a \approx 1.0$, deformation is controlled by diffusional creep and, when n_a is between 3.0 and 6.0, the dislocation power law mechanism controls creep deformation. The value of the activation energy Q_a is generally observed to be equal to the activation energy Q_d for self-diffusion. However, in most commercial creep-resistant alloys containing dispersed second-phase particles, the value of n_a and Q_a have been generally found to be considerably greater than those observed in pure metals and solid solution alloys [1–11]. The values of n_a for precipitation-hardened alloys usually appear to be between 5.0 and 15.0 [3–7] while, for dispersion-hardened alloys, n_a is in the range 10.0–40.0 [9, 10] and, for Ni–20Cr–2ThO_2 single crystals (where the composition is in approximate weight per cent), n_a is reported to be between 9.0 and 75.0 [11]. The value of the activation energy Q_a in some alloys has been found to be as high as three times the value of the activation energy Q_d for self-diffusion while in others is was nearly equal to the value of Q_d [8, 10, 12]. These variations in the observed values of n_a and Q_a have been rationalized by introducing the concept of a back stress or a threshold stress σ_0 which is an internal stress opposing the dislocation motion. With

*Present address: Beijing Institute for Aeronautical Materials, Beijing, China.

0025-5416/87/$3.50

this concept the steady state creep rate equation is modified to

$$\dot{\epsilon}_s = A^*\left(\frac{\sigma_a - \sigma_0}{G}\right)^{n_e} \frac{Gb}{kT} \exp\left(-\frac{Q_e}{RT}\right)$$

where $\sigma_a - \sigma_0$ is the effective applied stress, which is the driving force for dislocation glide, G is the shear modulus, b is the Burgers vector, k is the Boltzmann constant, Q_e is the effective activation energy of the creep process and is usually observed to be equal to Q_d, and n_e is the effective stress exponent. For pure metals, single-phase alloys and two-phase alloys the value of n_e has been observed to be equal to 1.0 for diffusional creep and to be between 3.0 and 6.0 for dislocation power law creep.

A number of studies of the creep mechanism for two-phase alloys have been carried out [4, 5, 13–17]. However, these studies on high temperature superalloys have been generally confined to the γ'-precipitation-hardened alloys. Therefore, research was initiated to study the creep deformation behaviour of γ''-precipitation-hardened superalloy Inconel 718. This alloy is precipitation hardened by approximately 13 vol.% of coherent ordered disc-shaped body-centred tetragonal γ'' phase and about 4 vol.% of spherical f.c.c. γ' phase precipitates in an f.c.c. matrix. Not only does it have an excellent room temperature strength but also it has a high resistance to creep deformation to temperatures above 900 K. The coarsening behaviour of γ'' and γ' particles and the room temperature deformation behaviour of this alloy have already been reported [18–20]. In this paper the mechanisms of creep deformation in the stress range 620–840 MN m^{-2} applied in a temperature range 853–943 K are presented.

2. MATERIAL AND EXPERIMENTAL TECHNIQUES

Sheets, 5 mm thick, of commercial alloy Inconel 718, whose chemical composition is shown in Table 1, were provided by the International Nickel Company of Canada. The as-received sheets of the material were cold rolled to 1.3 mm thickness. Flat tensile and creep specimens with a cross-section of 1.3 mm × 5.3 mm and a gauge length of 25.4 mm were machined from these strips. These specimens were given a final solution heat treatment at 1320 K for 1 h and quenched in iced water. They were then aged at 998 K for 15 h and quenched in iced water. In order to select appropriate creep stress levels, tensile tests were carried out at 873 and 923 K in an Instron testing machine. The creep tests were carried out in an argon atmosphere in two T48 Avery–Denison constant-stress creep machines. The creep strain was monitored during the tests by measuring the displacement with an extensometer attached to the specimen grips with a linear variable-differential transformer connected to a strip chart recorder. The creep rate was calculated by assuming that all the measured displacement was due to homogeneous deformation of the effective gauge length of the sample. The specimen temperature during creep tests was controlled to within ±2 K by using a three-zone furnace and was monitored by two thermocouples attached to the upper and lower gauge length portions of the test specimen. The back stress or threshold stress was determined by the Wilshire or the consecutive stress reduction method [4, 14, 15]. Details of this as well as of the microstructural examination techniques of aged and creep deformed specimens have been reported earlier [21].

3. RESULTS

The grain size of the heat-treated material was between 0.08 and 0.10 mm. Typical bright and dark field transmission electron microscopy (TEM) microstructures of the peak-aged specimens are shown in Fig. 1. The dark field micrograph was taken in the (001) orientation using a (001) reflection which coincided with both the γ'' and the γ' reflections. As reported earlier [18, 19], the disc-shaped particles are γ'' phase, and the spherical particles are γ' phase. Because of the presence of a high coherency strain around γ'' and γ' particles the precipitate particle sizes were measured from dark field micrographs. The average diameter of the γ'' discs and γ' particles in the peak-aged specimen was found to be 27.0 nm and 15.5 nm respectively. The

TABLE 1

Chemical composition of Inconel 718

Element	C	Fe	Ni	Cr	Al	Ti	Mo	Nb + Ta	Mn	S	Si	Cu
Amount (wt.%)	0.03	19.24	52.37	18.24	0.52	0.97	3.07	4.94	0.007	0.007	0.30	0.04

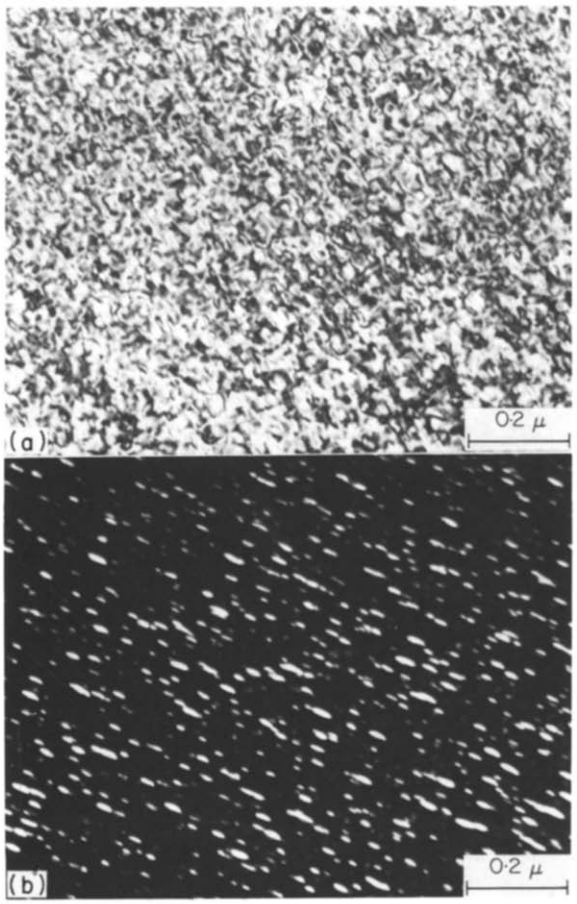

Fig. 1. Microstructure of a specimen aged for 15 h at 998 K: (a) bright field; (b) dark field taken with the (001) reflection spot.

tensile yield stresses of the material in this condition at 873 K and 923 K, at a strain rate of 3.3×10^{-4} s^{-1}, were 820 MN m^{-2} and 760 MN m^{-2} respectively. The creep tests were carried out in the temperature range 853-943 K and the stress range 620-840 MN m^{-2}. During these test conditions the material exhibited normal creep behaviour and, since only the secondary creep rates were of interest in this study, the tests were usually terminated before the initiation of tertiary creep.

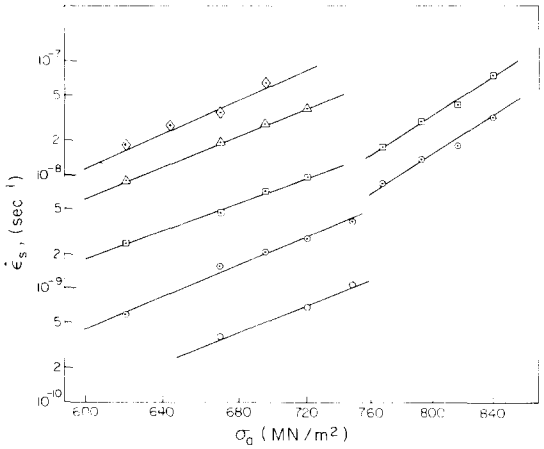

Fig. 2. Dependence of the steady state creep rate on the applied stress of specimens aged at 998 K for 15 h and tested at various temperatures for determining the values of n_a: ○, 853 K; ⊙, 873 K; ⊡, 898 K; △, 923 K; ◈, 943 K.

3.1. Apparent stress exponent n_a and effective stress exponent n_e

The dependence of creep rate on applied stress in the form of log $\dot{\epsilon}_s$-log σ_a plots in the stress ranges 620-746 MN m^{-2} and 765-840 MN m^{-2} at testing temperature of 853, 873, 898, 923 and 943 K is shown in Fig. 2. These plots suggest that a linear relationship exists between log $\dot{\epsilon}_s$ and log σ_a for the above testing conditions. The values of n_a calculated from the slopes of these plots and listed in Table 2 are similar to those observed in most creep resistant two-phase alloys, *i.e.* the values of n_a lie between 9.0 and 15.0. These values are considerably larger than the generally observed values of 1.0-6.0 for the creep of pure metals.

In two-phase alloys, creep does not take place under the full effect of applied stress σ_a but at a stress $\sigma_a - \sigma_0$, and it is considered that only the effective stress exponent n_e and effective activation energy Q_e determine the creep mechanism [3-5]. Therefore, to determine the effective stress exponents n_e and effective activation energy Q_e, the back stress

TABLE 2

Experimentally determined values of n_a, n_e and σ_0 (specimens aged for 15 h at 998 K with $d_{\gamma''} = 27.0$ nm and $d_{\gamma'} = 15.5$ nm)

Testing temperature (K)	σ_a (MN m^{-2})	σ_0 (MN m^{-2})	n_a	n_e
853	643, 670, 746	617	9.2 ± 0.6	1.2 ± 0.2
873	620, 670, 746	576	9.9 ± 0.8	1.4 ± 0.1
898	620, 670, 720	540	9.1 ± 0.5	1.6 ± 0.2
923	620, 670, 695	510	10.0 ± 0.8	2.3 ± 0.3
943	620, 670, 695	437, 460, 473	10.4 ± 1.4	5.9 ± 1.9
873	765, 815, 840	588, 605, 613	13.5 ± 1.0	5.1 ± 1.5
898	765, 815, 840	571, 582, 587	15.0 ± 1.5	5.9 ± 0.6

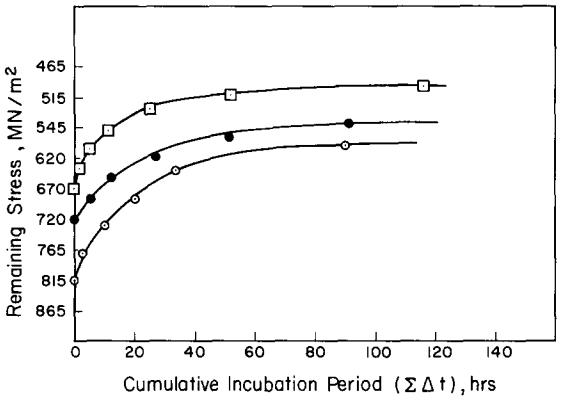

Fig. 3. Stress *vs.* cumulative incubation time $\Sigma\Delta t$ for specimens aged at 998 K for 15 h and tested at initial stresses of 815 MN m^{-2} at 873 K (⊙), 720 MN m^{-2} at 898 (●) and 670 MN m^{-2} at 923 K (⊡).

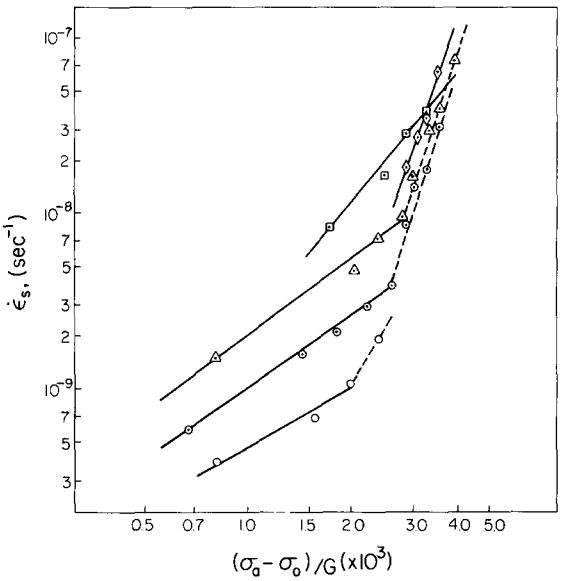

Fig. 4. Dependence of $\dot{\epsilon}_s$ on shear-modulus-compensated effective stress of the specimens aged at 998 K for 15 h and tested at various temperatures in the stress ranges 620–720 MN m^{-2} (——) and 765–840 MN m^{-2} (– – –), for determining the values of n_e: ○, 853 K; ⊙, 873 K; △, 898 K; ⊡, 923 K; ◇, 943 K.

and threshold stress σ_0 were measured by the consecutive stress reduction method. To determine the values of back stress, a few typical remaining stress *vs.* cumulative incubation period $\Sigma\Delta t$ curves are shown in Fig. 3 for temperatures of 873, 898 and 923 K. The back stress σ_0 was taken as the asymptotic value of remaining stress when the cumulative incubation time appeared to be infinite. The measured threshold stress and back stress σ_0 are listed in Table 2.

The values of the effective stress exponent n_e of the creep rate equation (eqn. (2)) were determined from the slopes of the plots of $\log \dot{\epsilon}_s$ *vs.* $\log\{(\sigma_a - \sigma_0)/G\}$. Figure 4 shows these plots for the specimens tested at temperatures in the range 853–943 K and at stresses in the range 620–840 MN m^{-2}. The values of n_e, as listed in Table 2, are observed to be in the range 1.2–5.9.

3.2. Apparent activation energy Q_a and effective activation energy Q_e

The apparent activation energies Q_a for the creep process were determined from the $\log \dot{\epsilon}_s$ *vs.* $1/T$ plots shown in Fig. 5. The calculated values, listed in Table 3, were found to be in the range from 355 ± 17 to 375 ± 13 kJ mol^{-1}. These values of apparent

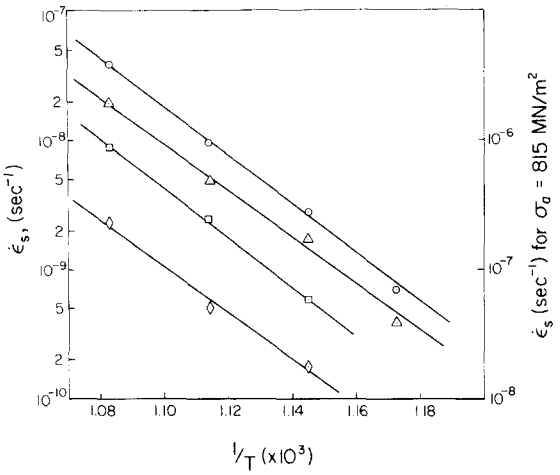

Fig. 5. Dependence of $\dot{\epsilon}_s$ on the reciprocal testing temperature $1/T$ of specimens aged at 998 K for 15 h and tested at various stress levels σ_a for determining the values of Q_a: ⊡, 620 MN m^{-2}; △, 670 MN m^{-2}; ⊙, 720 MN m^{-2}; ◇, 815 MN m^{-2}.

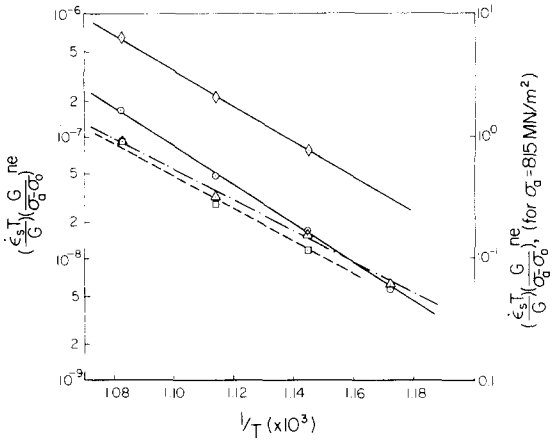

Fig. 6. Determination of the values of Q_e with inclusion of the variation in shear modulus with temperature and back stress for various stress levels σ_a: ⊡, - - -, 620 MN m^{-2}, △, —·—, 670 MN m^{-2}; ⊙, ——, 720 MN m^{-2}; ◇, —, 815 MN m^{-2}.

TABLE 3

Experimentally determined apparent and effective activation energies Q_a and Q_e ($d_{\gamma''}$ = 27.0 nm; $d_{\gamma'}$ = 15.5 nm)

σ_a (MN m^{-2})	Q_a (kJ mol^{-1})	Q_e (kJ mol^{-1})
620	375 ± 13	250 ± 8
670	355 ± 17	250 ± 13
720	368 ± 6	310 ± 8
815	360 ± 42	285 ± 12

activation energy are considerably greater than both the activation energy for self-diffusion and the activation energy for the creep process of pure nickel and Ni-Cr solid solution alloy. For example, the values of the activation energy for self-diffusion and the activation energy for the creep of nickel have been reported to be 265–280 kJ mol^{-1} and 276 kJ mol^{-1} respectively [22], and the activation energy for the creep of Ni-Cr solid solution alloy was found to be 295 kJ mol^{-1} [3] whereas the calculated values of Q_a were found to be between 355 and 375 kJ mol^{-1} (Table 3). However, the creep rate expression used to calculate these values considers neither the influence of temperature on the value of G nor the concept of back stress. Therefore the values of the effective activation energy Q_e were calculated from the creep rate equation [2], *i.e.* from the slope of the plots of $\ln[(\dot{\epsilon}_s T/G)\{G/(\sigma_a - \sigma_0)\}^{n_e}]$ *vs.* $1/T$. With Young's modulus values at 810 K and 920 K of 176 × 10^3 MN m^{-2} and 169 × 10^3 MN m^{-2} respectively [23, 24], Poisson's ratio ν of 0.33 and an n_e value of 1.0 at applied stress levels of 620, 670 and 720 MN m^{-2} and of 4.0 at an applied stress of 815 MN m^{-2}, the $\ln[(\dot{\epsilon}_s T/G)\{G/(\sigma_a - \sigma_0)\}^{n_e}]$ *vs.* $1/T$ plots are shown in Fig. 6. From the slopes of these plots the values of Q_e were found to be in the range from 250 ± 8 to 310 ± 8 kJ mol^{-1} and are listed in Table 3. These values of Q_e seem to be in a reasonable agreement with the activation energy for self-diffusion and the activation energies for the creep process of pure nickel and Ni-Cr solid solution alloys, as quoted earlier.

4. DISCUSSION

The experimental results given in Table 2 show that the value of the effective stress exponent n_e increases as either the testing temperature or the applied stress increases in the testing regime used in the investigation. In the low stress range 620–720 MN m^{-2}, the value of n_e increases from 1.2 ± 0.2 at 853 K to 5.9 ± 1.9 at 943 K, suggesting that the creep mechanism changes from diffusional or linear creep to dislocation power law creep as the temperature increases from 853 to 943

K. However, in the stress range 765–840 MN m^{-2}, the power law creep mechanism operates at temperatures of both 873 and 898 K. The results given in Table 2 also show that at 873 K the value of n_e changes from 1.4 ± 0.1 in the stress range 620–746 MN m^{-2} to 5.10 ± 1.5 in the stress range 765–840 MN m^{-2}. For a testing temperature of 898 K, the value of the effective stress exponent changes from 1.6 ± 0.2 at the low stress level of 620–720 MN m^{-2} to 5.9 ± 0.6 at the high stress level of 765–840 MN m^{-2}. This suggests that the creep mechanism changes from diffusional creep or linear creep to dislocation power law creep when the applied stress σ_a increases from 620–720 MN m^{-2} to 765–840 MN m^{-2} in the temperature range 873–898 K.

The results of the present study also show that the value of n_e are not exactly equal to 1.0 but are slightly greater than 1.0 in the low stress range 620–720 MN m^{-2} and the temperature range 853–873 K, where creep is considered to be diffusion controlled. This slightly higher value of n_e may be attributed to the following reasons. The mechanism of diffusional creep of two-phase alloys is different from that of single-phase alloys or pure metals. Diffusional creep in the latter is known to be the result of stress-induced diffusion or the migration of matter from grain boundaries that are in tension to those in compression. The flow of vacancies during this stage is in the reverse direction. The accumulation of diffusing vacancies leads to grain boundary sliding, and dislocation motion inside the grain is not involved. In contrast, in two-phase alloys, diffusion of vacancies will be inhibited by the precipitate particles with an accumulation of vacancies at the precipitate–matrix interface and a resultant build-up of stress concentration. This stress concentration at the interface can only be relaxed by the punching of prismatic dislocation loops in the matrix, which can annihilate themselves by the absorption of vacancies [16, 17]. Therefore, to accommodate even very limited diffusional strain in two-phase alloys, additional plastic deformation must occur around precipitates either in the grain boundary region or within grains, giving an n_e value slightly greater than 1.0. Furthermore, according to Ansell and Weertman [25], diffusional creep can involve the process of dislocation climb over the particles. Therefore, diffusional creep in two-phase alloys can involve not only vacancy diffusion in the matrix and dislocation motion in the grain boundary region but also dislocation creation and motion within the grains. Ansell and Weertman assume the rate-controlling process to be the climb of dislocations over the precipitate particles which also depends on the diffusion rate. However, if cross-slip is also important in the above process, the creep rate will be more sensitive to stress. In the present investigation the microstructures of crept specimens showed that dislocation segments and loops do exist within grains even under the testing conditions where diffusional creep is considered to occur. Examples of this are illustrated in Fig. 7, which is the microstructure of a specimen aged at 998 K for 15 h and tested 873 K at a stress of 720 MN m^{-2} for 222 h. These observations suggest that the creep is more sensitive to the applied stress in two-phase alloys than to that in pure metals, *i.e.* the value of n_e can be slightly greater than 1.0. This observation is in agreement with the findings of Ansell and Weertman [25].

Diffusional creep in two-phase alloys has three additional characteristics.

(1) The creep rate decreases with time or total strain, *i.e.* there exists a limiting total creep strain ϵ_l [16, 17].

(2) There is a threshold stress below which $\dot{\epsilon}_s \to 0$, *i.e.* the value of σ_0 is constant [16, 17].

(3) There are precipitate-free zones (PFZs) around grain boundaries in tension during creep deformation [1].

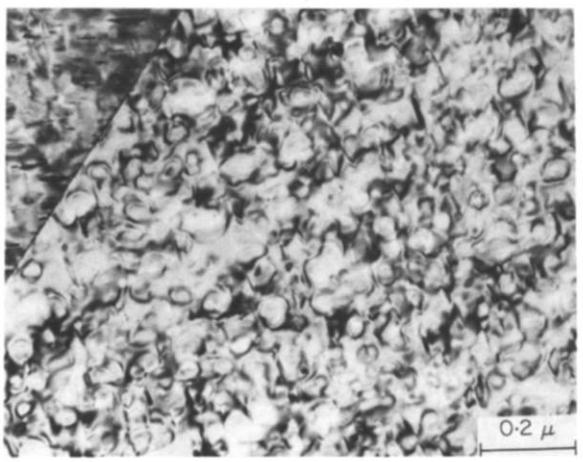

Fig. 7. Dislocation structure of a specimen aged for 15 h at 998 K and crept at 873 K under 720 MN m^{-2} for 222 h.

In the regime where the value of n_e is nearly equal to 1.0, the applicability of the above criteria were also examined. For this purpose a few creep tests, for which the value of n_e was nearly equal to 1.0, were conducted for a prolonged time (more than 150 h) to determine the variation in creep rate $\dot{\epsilon}_s$ with time. The results, typically as shown in Fig. 8, suggest that the value of $\dot{\epsilon}_s$ decreases with time or total strain, and finally the creep rate approaches a limiting value in accordance with criterion (1) of diffusional creep listed above. It was also observed that in the low stress range 620–720 MN m^{-2} and at a temperature below 873 K, where the value of n_e is nearly equal to 1.0, the value of σ_0 was nearly constant; this is an accordance with criterion (2) of diffusional creep listed above.

Harris [16] and Burton [17] have suggested that the diffusional creep rate of two-phase alloys depends on the ability of grain boundaries to collect precipitates. When a two-phase material undergoes creep deformation, the precipitates are progressively collected on compressive grain boundaries and hence their ability to collect precipitates decreases with total strain, *i.e.* the creep rate decreases with time. This model suggests that a PFZ should be present around grain boundaries that are in tension when a creep test lasts for a sufficiently long time. According to Harris [16] and Gittus [26], the total limiting creep strain ϵ_1 under this condition is equal to $2x/d$ where x is the width of the PFZ around grain boundaries under tension and d is the grain size. There should not be any PFZ around those grain boundaries that are in compression. It can be assumed that the width of the PFZ around grain boundaries that are neither perpendicular nor parallel to the stress axis will be proportional to the angle of the orientation between the applied stress axis and grain boundary. In the present investigation, it was observed that, when the peak-aged specimen with $d_{\gamma''} = 27$ nm was tested at 873 K and at a stress of 720 MN m^{-2} for 222 h, the total limiting strain ϵ_1 was about 0.15%. For a specimen in the over-aged condition with $d_{\gamma''} = 54$ nm tested at a stress 695 MN m^{-2} and a temperature of 873 K for 403 h, its value was nearly 0.5%. In these two cases the calculated widths of PFZ around grain boundaries in tension should be about 75 nm and 250 nm respectively when the grain size is about 0.1 mm. A PFZ of such a narrow width cannot be observed with an optical microscope and must be observed with an electron microscope. Occasionally by TEM studies the presence of a PFZ was detected in creep deformation studies, which was not observed in as-aged material. An example of such a PFZ is shown in Fig. 9 which is the TEM micrograph of a specimen aged for 25 h at 998 K and creep deformed for 222 h at 873 K at an applied stress of 720 MN m^{-2}. The width of the PFZ is observed to be about 40 nm which compares reasonably with the theoretically estimated value of 75 nm. Therefore, it may be concluded that the creep deformation of Inconel 718 under low stress and temperature conditions occurs by the diffusional or linear creep mechanism.

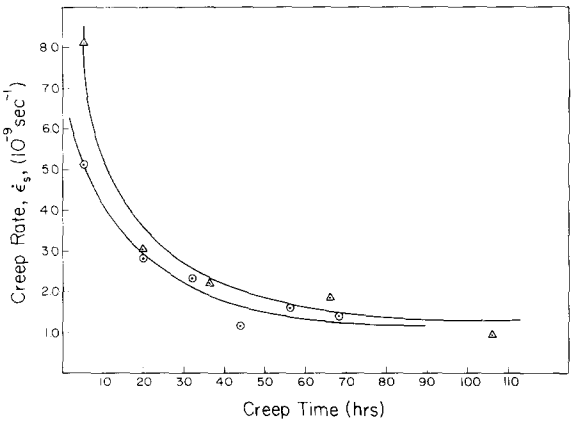

Fig. 8. Dependence of the creep rate on the creep time of specimens crept at 873 K under a stress of 720 MN m^{-2}: ⊙, aged for 15 h at 998 K; △, aged for 25 h at 998 K.

The existence of a transition region between diffusional creep and homogeneous power law creep has been suggested by Ashby and Frost [27]. They considered diffusional flow as grain boundary sliding with diffusional accommodation. During this process, incompatibility generated by grain boundary sliding is removed at a steady rate by diffusion of atoms from sources on some grain boundaries to sinks on others. If the strain rate is increased sufficiently, diffusion can no longer accommodate the sliding and a non-uniform power law creep within grains, called "folds", appears. As the strain rate increases further, flow becomes increasingly uniform and the folds disappear. This process leads to homogeneous power law creep. The region where

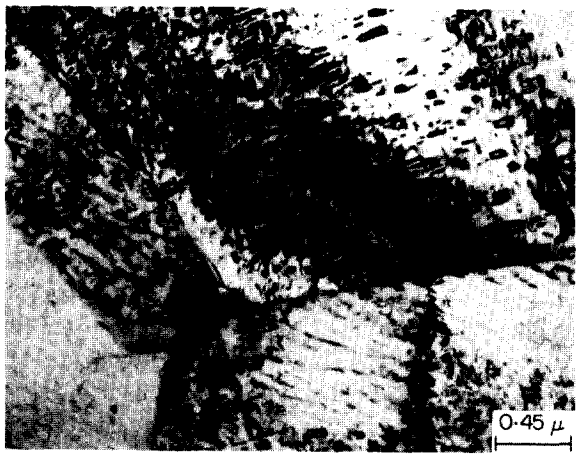

Fig. 9. TEM micrograph of a specimen aged for 25 h at 998 K and creep deformed at 873 K at a stress of 720 MN m^{-2} for 222 h, showing the presence of a PFZ around one of the grain boundaries.

diffusion can no longer accommodate the grain boundary sliding and non-uniform power law creep appears is designated as a "transition region" between diffusional and power law creep. The results, presented in Table 2, show that the value of n_e changes continuously from 1.2 ± 0.2 to 5.9 ± 1.9 when the testing temperature is increased from 853 to 943 K. Therefore, although the results of the present study are limited in this regard, they do suggest the existence of a transition region between the diffusion and power law creep regions in Inconel 718 which is in accordance with the suggestion of Ashby and Frost [27].

5. CONCLUSIONS

(1) For the testing conditions employed, *i.e.* a temperature range from 853 to 943 K and an applied stress range from 620 to 865 MN m^{-2}, the values of the apparent stress exponent n_a and the activation energy Q_a for the creep rate equation

$$\dot{\epsilon}_s = A\sigma_a{}^{n_a} \exp\left(-\frac{Q_a}{RT}\right)$$

were between 9.1 and 15.0 and between 355 and 375 kJ mol^{-1} respectively. The value of effective stress exponent n_e and activation energy Q_e for the creep rate equation

$$\dot{\epsilon}_s = A^* \frac{Gb}{kT}\left(\frac{\sigma_a - \sigma_0}{G}\right)^{n_e} \exp\left(-\frac{Q_e}{RT}\right)$$

were between 1.2 and 5.9 and between 250 and 310 kJ mol^{-1} respectively.

(2) The value of the effective stress exponent and the activation energy suggest that the creep deformation mechanism of Inconel 718 alloy changes from linear or diffusional creep ($n_e \approx 1.0$) to dislocation power law creep ($n_e \approx 3.0$–6.0) when the temperature or applied stress is increased. The experimental results also suggest that there is a transition region between the diffusional creep and the dislocation power law creep regions. This transition is attributed to the occurrence of non-uniform power law creep within the grains as the temperature or applied stress is changed from the linear law creep region to the dislocation power law creep region.

ACKNOWLEDGMENTS

The authors would like to express their appreciation to Dr. Cahoon for many useful discussions, the International Nickel Company of Canada for supplying the materials and the Natural Science and Engineering Research Council of Canada for financial support. One of the authors (Y. H.) would like to express her thanks to the University of Manitoba, Canada, for the award of a graduate fellowship and the Institute of Aeronautical Materials, Beijing, China, for giving her leave of absence.

REFERENCES

1 D. D. Sherby and P. M. Burke, *Prog. Mater. Sci., 13* (1967) 325.
2 D. McLean, *Rep. Prog. Phys., 29* (1966) 1.
3 D. Sidey and B. Wilshire, *Met. Sci. J., 3* (1969) 56.
4 K. Williams and B. Wilshire, *Met. Sci. J., 7* (1973) 176.
5 J. D. Parker and B. Wilshire, *Met. Sci. J., 9* (1975) 248.
6 R. Lagneborg and B. Bergman, *Met. Sci. J., 10* (1976) 20.
7 W. J. Evans and G. F. Harrison, *Met. Sci. J., 10* (1976) 307.
8 C. L. Meyers, J. C. Shyne and O. D. Sherby, *J. Aust. Inst. Met., 8* (1963) 171.
9 B. A. Wilcox and A. H. Clauer, *Trans. Metall. Soc. AIME, 236* (1966) 570.
10 A. H. Clauer and B. A. Wilcox, *Met. Sci. J., 1*

(1967) 86.
11 R. W. Lund and W. D. Nix, *Acta Metall., 24* (1976) 469.
12 B. A. Wilcox and A. H. Clauer, *Met. Sci. J., 3* (1969) 26.
13 C. Carry and J. L. Strudel, *Acta Metall., 25* (1977) 767.
14 P. W. Davies, G. Nelmes, K. R. Williams and B. Wilshire, *Met. Sci. J., 7* (1973) 87.
15 J. D. Parker and B. Wilshire, *Met. Sci. J., 12* (1978) 453.
16 J. E. Harris, *Met. Sci. J., 7* (1973) 1.
17 B. Burton, *Mater. Sci. Eng., 11* (1973) 337.
18 Y. Han, P. Deb and M. C. Chaturvedi, *Met. Sci. J., 16* (1982) 555.
19 M. C. Chaturvedi and Y. Han, *Met. Sci. J., 17* (1983) 145.
20 Y. Han, *Master's Thesis*, University of Manitoba, Canada, 1982.
21 Y. Han and M. C. Chaturvedi, A study of back stress during creep deformation of Inconel 718, *Mater. Sci. Eng., 85* (1987) 59–65.
22 J. P. Dennison, R. J. Llewellyn and B. Wilshire, *J. Inst. Met., 95* (1967) 115.
23 *Metals Handbook*, Vol. 3, American Society for Metals, Metals Park, OH, 9th edn., 1980, pp. 242–268.
24 C. T. Sims and W. C. Hagel, *The Superalloys*, Wiley, New York, 1972, p. 602.
25 G. S. Ansell and J. Weertman, *Trans. Metall. Soc. AIME, 215* (1959) 838.
26 J. Gittus, *Creep Viscoelasticity and Creep Fracture in Solids*, Applied Science, London, 1975, pp. 14–41.
27 M. F. Ashby and H. J. Frost, in A. S. Argon (ed.), *Constitutive Equations in Plasticity*, Massachusetts Institute of Technology Press, Cambridge, MA, 1975, p. 117.